Gap Function with Point Nodes in Borocarbide Superconductor YNi_2B_2C

K. Izawa,[1] K. Kamata,[1] Y. Nakajima,[1] Y. Matsuda,[1] T. Watanabe,[2] M. Nohara,[3] H. Takagi,[3] P. Thalmeier,[4] and K. Maki[5]

[1]*Institute for Solid State Physics, University of Tokyo, Kashiwa, Chiba 277-8581, Japan*
[2]*Department of Applied Chemistry, University of Tokyo, Bunkyo-ku, Tokyo 113-8656, Japan*
[3]*Department of Advanced Materials Science, University of Tokyo, Bunkyo-ku, Tokyo 113-0033, Japan*
[4]*Max-Planck-Institute for the Chemical Physics of Solid, Nöthnitzer Strasse 40, 01187 Dresden, Germany*
[5]*Max-Planck-Institute for the Physics of Complex Systems, Nöthnitzer Strasse 38, 01187 Dresden, Germany*

(Received 8 May 2002; published 9 September 2002)

To determine the superconducting gap function of YNi_2B_2C, the c-axis thermal conductivity κ_{zz} was measured in $\boldsymbol{H}$ rotated in various directions. The angular variation of κ_{zz} in $\boldsymbol{H}$ rotated within the ab plane shows a peculiar fourfold oscillation with narrow cusps. The amplitude of this fourfold oscillation becomes very small when $\boldsymbol{H}$ is rotated conically around the c axis with a tilt angle of 45°. These results provide the first compelling evidence that the gap function has *point nodes* located along the a and b axes. This unprecedented gap structure challenges the current view on the pairing mechanism.

DOI: 10.1103/PhysRevLett.89.137006 PACS numbers: 74.20.Rp, 74.25.Fy, 74.25.Jb, 74.70.Dd

In the past two decades, unconventional superconductivity with different symmetry other than s-wave symmetry has been found in heavy fermion materials [1], high-T_c cuprates [2], ruthenate [3], and organic compounds [4]. Unconventional superconductivity is characterized by anisotropic gap functions belonging to nontrivial representations of the symmetry group which may have zeros (nodes) along certain crystal directions. Since the nodal structure is ultimately related to the pairing interaction, its identification is crucial for understanding the pairing mechanism. A common feature in the unconventional superconductors discovered until now is that they all have *line nodes* in the gap functions, which are located parallel or perpendicular to the basal planes. It is generally believed that these nodal structures appear as a result of pairing interactions caused by purely electronic origin, instead of being mediated by conventional phonons.

It is well known that there can be another type of gap singularity, i.e., point node in which the gap turns to zero at isolated points on the Fermi surface. The point node is present in the A and A_1 phases of superfluid ^{3}He. On the other hand, its existence has never been reported in any superconductor so far except for the B phase of UPt_3 in which a possibility of the point nodes coexisting with line nodes was suggested theoretically [5]. Thus, it is still an open question whether a superconductor can really have point nodes, and its clarification is an important subject for the study of the unconventional superconductivity.

In this Letter, we direct our attention to a new class of superconductors, nonmagnetic borocarbide superconductors LNi_2B_2C, L = (Y and Lu) [6] with 3D and tetragonal electronic structure. At an early stage, the gap symmetry of these materials was considered to be isotropic s wave, mediated by conventional electron-phonon interactions [7]. However, recent specific heat [8,9], thermal conductivity [10], Raman scattering [11], and photoemission spectroscopy [12] experiments on YNi_2B_2C or $LuNi_2B_2C$ have reported a large anisotropic gap function. Despite these studies, the detailed structure of the gap function remains unknown. Here, we provide strong evidence that the gap function of YNi_2B_2C has *point nodes,* which are located along the [100] and [010] directions. These results are based on the angular variation of the thermal transport in a magnetic field rotated in various directions relative to the crystal axes, which has proved to be a powerful probe for determining the low energy quasiparticle (QP) excitation including its direction [13–21]. This unprecedented gap structure challenges the current view on the mechanism of the superconductivity and on the many unusual superconducting properties of borocarbide superconductors [7,22].

Single crystals of YNi_2B_2C (T_c = 15.5 K) were grown by the floating zone method. The residual resistivity ratio was approximately 47, indicating the highest crystal quality currently achievable. We measured the c-axis thermal conductivity κ_{zz} (the heat current $\boldsymbol{q} \parallel c$) on the sample cut into a rectangular shape ($0.31 \times 0.54 \times 3.00$ mm^3) by the steady-state method. To apply $\boldsymbol{H}$ with high accuracy (misalignment of less than 0.02°) relative to the crystal axes, we used a system with two superconducting magnets generating $\boldsymbol{H}$ in two mutually orthogonal directions and a ^{3}He cryostat equipped on a mechanical rotating stage at the top of the Dewar [15,16].

Figure 1(a) shows the T dependence of κ_{zz} in zero field. At T_c, κ_{zz} exhibits a tiny kink. In this temperature range, the electronic contribution well dominates over the phonon contribution. The inset of Fig. 1(a) shows the same data below 1 K. The T dependence of κ_{zz} is close to quadratic rather than cubic. Figure 1(b) depicts the H dependence of κ_{zz} ($\boldsymbol{H} \parallel$ [110]). At low field κ_{zz} increases rapidly with H. This steep increase is markedly different from that observed in the s-wave superconductors in

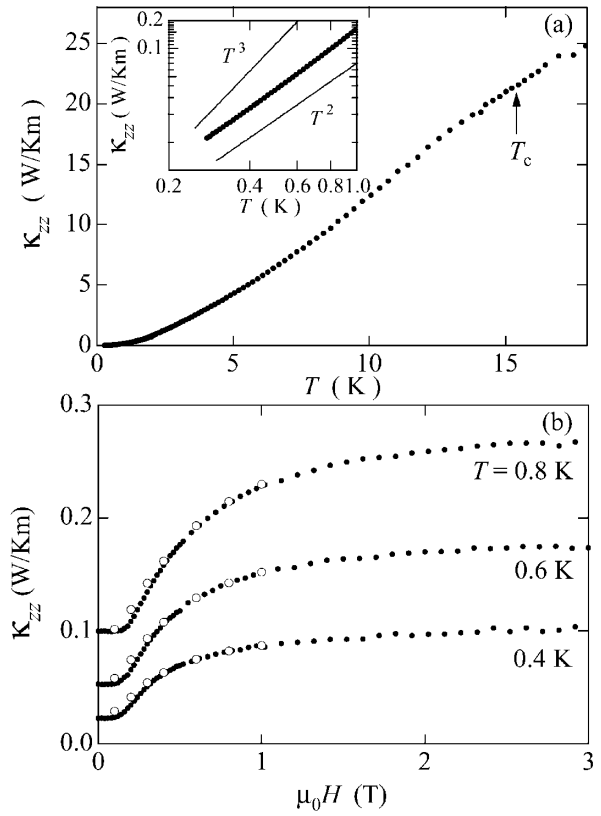

FIG. 1. (a) T dependence of κ_{zz} in zero field. Inset: Log-log plot of the same data below 1 K. (b) Field dependence of κ_{zz} at low temperatures ($\boldsymbol{H} \parallel [110]$). The solid circles represent the data measured by sweeping H after zero field cooling, and the open circles represent the data measured under the field cooling conditions at each temperature.

which the thermal conductivity shows an exponential behavior with much slower growth with H at $H \ll H_{c2}$. Similar H dependence has been reported in $LuNi_2B_2C$ [10]. The steep increase of the thermal conductivity, along with the $\sqrt{H}$ dependence of the heat capacity [8,9], are evidence that the thermal properties are governed by the delocalized QPs arising from the nodes in the gap function. The theoretical understanding of the heat transport for superconductors with nodes has largely progressed during the past few years [23]. The most remarkable effect on the thermal transport is the Doppler shift of the energy of a QP with momentum $\boldsymbol{p}$ [$E(\boldsymbol{p}) \rightarrow E(\boldsymbol{p}) - \boldsymbol{v}_s \cdot \boldsymbol{p}$] in the circulating supercurrent flow $\boldsymbol{v}_s$ [24]. This effect becomes important at such positions where the local energy gap becomes smaller than the Doppler shift term ($\Delta < \boldsymbol{v}_s \cdot \boldsymbol{p}$), which can be realized in the case of superconductors with nodes. This effect gives rise to a finite density of states (DOS) at the Fermi surface, which in turn causes a steep increase of the thermal conductivity with H.

Having established the predominant contribution of the delocalized QPs in the thermal transport, the next question is the nodal structure. The important advantage of choosing to measure the thermal conductivity is that it is a *directional* probe for the nodal directions of the order parameter [13–21]. This is because the magnitude of the Doppler shift is sensitive to the relative orientation between $\boldsymbol{H}$ and node. For instance, when $\boldsymbol{H}$ is rotated within the basal plane in 2D d-wave superconductors, the DOS shows the maximum (minimum) when $\boldsymbol{H}$ is applied to the antinodal (nodal) directions. As a result, a clear fourfold modulation of the thermal conductivity, which reflects the angular position of line nodes of d-wave symmetry, has been observed in high-T_c cuprate $YBa_2Cu_3O_{7-\delta}$ [13,14], heavy fermion $CeCoIn_5$ [15], and organic κ-$(ET)_2Cu(NCS)_2$ [16].

Figure 2 displays the angular variation of κ_{zz}, which was measured by rotating $\boldsymbol{H} = H(\sin\theta\cos\phi, \sin\theta\sin\phi, \cos\theta)$ conically as a function of ϕ, keeping θ constant. Here $\theta = (\boldsymbol{q}, \boldsymbol{H})$ is the polar angle and ϕ is the azimuthal angle measured from the a axis (see the inset of Fig. 2). The crosses in Fig. 2 show $\kappa_{zz}(H, \phi)$ at $H = 1$ T which are obtained under the field cooling condition at each angle. $\kappa_{zz}(H, \phi)$ obtained by different procedures well coincide with each other, indicating that the field trapping effect is negligibly small at $H = 1$ T. A clear fourfold symmetry is observed at $\theta = 90°$ and 60°; κ_{zz} can be decomposed as $\kappa_{zz} = \kappa_{zz}^0 + \kappa_{zz}^{4\phi}$, where κ_{zz}^0 is a ϕ-independent term and $\kappa_{zz}^{4\phi}$ is a term with fourfold symmetry with respect to ϕ rotation. Similar results were obtained at 0.27 and 0.8 K. We note that in the

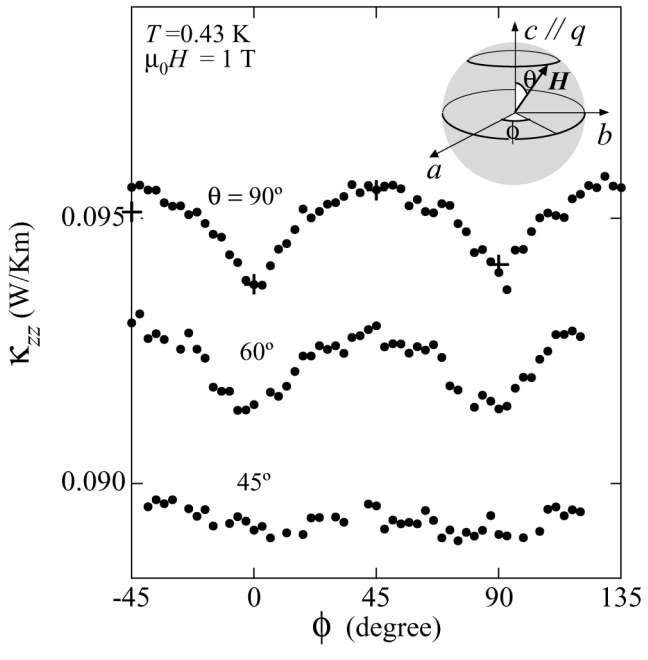

FIG. 2. Angular variation of κ_{zz} at $H = 1$ T and $T = 0.43$ K ($\boldsymbol{q} \parallel c$). κ_{zz} are measured by rotating $\boldsymbol{H} = H(\sin\theta\cos\phi, \sin\theta\sin\phi, \cos\theta)$ conically as a function of ϕ at fixed $\theta = 90°$, 60°, and 45° (see the inset). The crosses represent the data obtained under the field cooling condition at each angle.

previous measurements in which the in-plane thermal conductivity κ_{xx} was measured in $\boldsymbol{H}$ rotating within the ab plane, a large twofold term appears as a result of the difference of the effective DOS for QPs traveling parallel to the vortex and for those moving in the perpendicular direction [13–16]. In the present geometry, on the other hand, such a twofold term is absent because κ_{zz} was measured in keeping θ constant [19].

As seen in Fig. 2, $\kappa_{zz}^{4\phi}$ shows a peculiar angular variation. The first point to emphasize is the appearance of a narrow cusp at $\phi = 0°$ and 90°. This angular variation is markedly different from those in d-wave superconductors with line nodes, in which such a cusp structure is absent [13–16]. The second point is that the amplitude of $\kappa_{zz}^{4\phi}$ decreases rapidly as $\boldsymbol{H}$ is changed from $\theta = 90°$ to 45°. Here we stress that the fourfold anisotropies of the Fermi velocity v_F and H_{c2}, which are inherent to the tetragonal band structure of YNi_2B_2C, are quite unlikely to be an origin of $\kappa_{zz}^{4\phi}$ for the following reasons. The ϕ dependence of H_{c2} both at $\theta = 90°$ and 45° shows nearly perfect sinusoidal ϕ dependence with fourfold symmetry, similar to H_{c2} of $LuNi_2B_2C$ [25]. This is totally different from the ϕ dependence of $\kappa_{zz}^{4\phi}$ displayed in Fig. 2. In addition, the amplitude of fourfold oscillation of H_{c2} at $\theta = 45°$ was nearly 1/3 of that at $\theta = 90°$, while the amplitude of $\kappa_{zz}^{4\phi}$ at $\theta = 45°$ is less than 1/5 of that at $\theta = 90°$, indicating a different θ dependence of two quantities. Moreover, according to the calculation based on the Kubo formula, the leading term in $\kappa_{zz}^{4\phi}$ is the anisotropy of the gap function and anisotropy of v_F will enter only as a secondary effect. These considerations lead us to conclude that *the observed fourfold symmetry originates from the gap nodes*.

We are now in a position to discuss the detailed nodal structure. The fact that $\kappa_{zz}^{4\phi}$ shows the minimum at $\phi = 0°$ and 90° immediately indicates that *the nodes are located along the [100] and [010] directions*. In the following, we show that the $\kappa_{zz}^{4\phi}$ is sensitive to the gap function; the cusp structure and θ dependence of $\kappa_{zz}^{4\phi}$ are

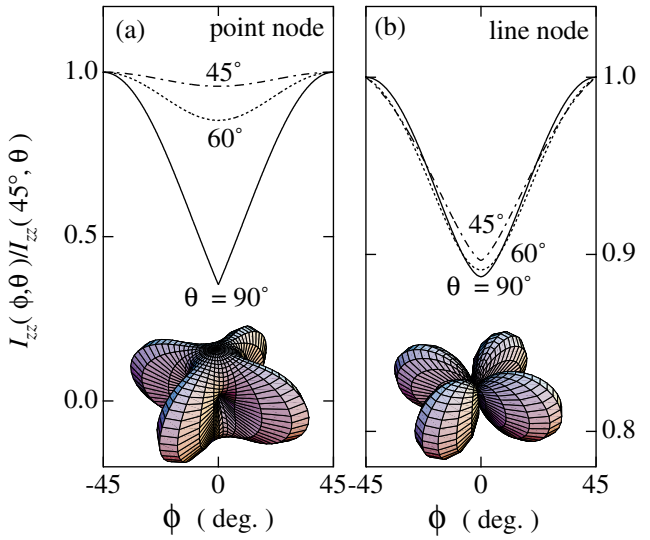

FIG. 3 (color). Angular variation of $I_{zz}(\phi, \theta)$ normalized by $I_{zz}(45°, \theta)$ as a function of ϕ at $\theta = 90°$ (solid lines), 60° (dashed lines), and 45° (dash-dotted lines), which are calculated by the gap functions with (a) point node and (b) line node. For the definition of θ and ϕ, see the inset of Fig. 2. The corresponding gap functions are illustrated in the insets. For details, see the text.

key features for specifying the type of nodes. In Figs. 3(a) and 3(b), we compare $\kappa_{zz}^{4\phi}$ for two different types of nodes calculated from the Doppler-shifted QP spectrum. Here we adopted gap functions $\Delta(\boldsymbol{k}) = \frac{1}{2}\Delta_0\{1 - \sin^4\theta\cos(4\phi)\}$ proposed in Ref. [20] for point node, and $\Delta(\boldsymbol{k}) = \Delta_0\sin(2\phi)$ (d wave) for the line node [26] (see the insets in Figs. 3). $\kappa_{zz}(H, \phi, \theta)$ is given as [21]

$$\frac{\kappa_{zz}}{\kappa_n} = \frac{1}{6\sqrt{2}\pi}\left(\frac{v_a v_c \hbar e H}{\Delta^2 c}\right)^{3/2} I_{zz}(\phi, \theta), \tag{1}$$

where $v_{a,c}$ are the anisotropic Fermi velocities. For point nodes, I_{zz} is given as $I_{zz}(\phi, \theta) = I_+(\phi, \theta)^3$ and

$$I_+(\phi, \theta) = \tfrac{1}{2}[\{1 + \cos^2\theta + \sin^2\theta\cos(2\phi)\}^{1/2} + \{1 + \cos^2\theta - \sin^2\theta\cos(2\phi)\}^{1/2}]. \tag{2}$$

For the line nodes, I_{zz} is given as $I_{zz}(\phi, \theta) = I_+(\phi, \theta)^2$ and

$$I_+(\phi, \theta) = \frac{1}{2\pi}\int_{-\pi/2}^{\pi/2} d\psi\Bigg[\left\{1 + \frac{1}{2}\sin^2\theta(\cos(2\phi) - \cos(2\psi)) + \frac{1}{\sqrt{2}}\sin(2\theta)\sin\psi\sqrt{1 - \sin(2\theta)}\right\}^{1/2} + \left\{1 - \frac{1}{2}\sin^2\theta(\cos(2\phi) + \cos(2\psi)) + \frac{1}{\sqrt{2}}\sin(2\theta)\sin\psi\sqrt{1 + \sin(2\theta)}\right\}^{1/2}\Bigg]. \tag{3}$$

Here, the superclean limit $\frac{\hbar\Gamma}{\Delta} \ll \frac{H}{H_{c2}}$ is assumed, where Γ is the carrier scattering rate which is estimated to be $\hbar\Gamma < 1$ K. Using $\Delta \simeq 28$ K, $H_{c2} \simeq 10$ T, the superclean condition is well satisfied. We first compare $\kappa_{zz}^{4\phi}$ at $\theta = 90°$. A clear narrow cusp structure is seen at $\phi = 0°$ and 90° for the point node, while it is absent and $\kappa_{zz}^{4\phi}$ is close to the sinusoidal wave for the line node. Qualitatively, this can be explained as the following. The narrow cusp in $\kappa_{zz}^{4\phi}$ appears as a result of the smaller freedom of the QPs induced in the vicinity of point nodes. On the other hand, the cusp structure is smeared out due to the larger freedom associated with the line node. We next discuss how the amplitude of $\kappa_{zz}^{4\phi}$ changes with θ. For point nodes, the amplitude of $\kappa_{zz}^{4\phi}$ at $\theta = 45°$ is much smaller than that at $\theta = 90°$, while they are of almost the same magnitude

for line nodes. This can be accounted for by considering the fact that rotating $\boldsymbol{H}$ conically at $\theta = 45°$ does not point to the nodes in the case of the point nodes, while rotating $\boldsymbol{H}$ at any θ always cross the nodes in the case of the line nodes. It is apparent that both the cusp structure and θ dependence of $\kappa_{zz}^{4\phi}$ shown in Fig. 3(a) are strongly in favor of the point nodes. We have calculated $\kappa_{zz}^{4\phi}$ for different types of gap functions with point nodes and found that both the cusp structure and the θ dependence of $\kappa_{zz}^{4\phi}$ are robust for the choice of the gap functions. In addition, we have measured the in-plane thermal conductivity ($\boldsymbol{q} \parallel [110]$) of a different crystal in $\boldsymbol{H}$ rotated within the [110] plane and found no anomaly associated with the point node along the [001] direction. These results lead us to our aforementioned conclusion that the gap function of YNi_2B_2C has *point nodes* which are located along the [100] and [010] directions.

In the present experiment, we cannot rule out the possibility that there remains a very small but finite gap at the nodal positions. Let us estimate the upper limit of the gap anisotropy ratio $\Delta_{\min}/\Delta_{\max}$, where $\Delta_{\max}$ and $\Delta_{\min}$ are the gap maximum and minimum, respectively. The fact that the clear fourfold pattern characteristic to the point node was observed even at $T = 0.27$ K suggests that $\Delta_{\min}$ is much less than 0.27 K. Assuming the weak coupling BCS relation for the maximum gap ($\Delta_{\max} = 1.75 k_B T_c$), we obtain $\Delta_{\min}/\Delta_{\max} < 0.01$ at 0.5 T; *the gap is highly anisotropic.* According to Refs. [8,12], the introduction of nonmagnetic impurity in YNi_2B_2C reduces the DOS at the Fermi surface by removing the node. This indicates that the gap function does not change its sign at the nodes, because otherwise the impurity always induces a finite DOS at the Fermi level [27]. Therefore, the impurity effect is consistent with the point node for which case the gap function does not change its sign at the node.

Various authors have pointed out that calculations based on the Eliashberg equation reproduces well the high transition temperature of LNi_2B_2C in terms of the observed phonon spectrum and isotropic gap [7]. However, the determined gap structure with point nodes casts doubt on such a view based on a simple phonon mediated pairing mechanism. At the present stage, what kind of interaction gives rise to the point node is not known. We also point out that this nodal structure should play an important role in determining the superconducting properties, such as the vortex lattice structure, reversible magnetization, and H_{c2}, which have been discussed in terms of the nonlocal London theory assuming an ordinary s-wave superconductor until now [22]. We believe the present study motivates further investigations on these subjects. For instance, the extended QPs appear to be important for the vortex lattice phase transition [28].

In summary, we present the first compelling evidence that the gap function of YNi_2B_2C has *point nodes* which are located along the [100] and [010] directions. To the best of our knowledge, YNi_2B_2C (and presumably $LuNi_2B_2C$) is the first superconductor in which the gap function with the point nodes was successfully identified. The determined gap structure offers a new perspective on the pairing mechanism as well as unusual superconducting properties of anisotropic superconductors.

We thank D. F. Agterberg, T. Dahm, V. Kogan, K. Machida, P. Miranovic, M. Sigrist, A. Tanaka, K. Ueda, and I. Vekhter for stimulating discussions.

[1] M. Sigrist and K. Ueda, Rev. Mod. Phys. **63**, 239 (1991).
[2] C. C. Tsuei and J. R. Kirtley, Rev. Mod. Phys. **72**, 969 (2000).
[3] Y. Maeno, T. M. Rice, and M. Sigrist, Phys. Today **54**, No. 1, 42 (2001).
[4] K. Kanoda, Physica (Amsterdam) **282C–287C**, 299 (1997).
[5] M. J. Graf, S. K. Yip, and J. A. Sauls, Phys. Rev. B **62**, 14 393 (2000).
[6] P. C. Canfield, P. L. Gammel, and D. L. Bishop, Phys. Today **51**, No. 10, 40 (1998).
[7] S. A. Carter *et al.*, Phys. Rev. B **50**, 4216 (1994); L. F. Mattheiss, *ibid.* **49**, 13 279 (1994); H. Michor *et al.*, *ibid.* **52**, 16 165 (1995); R. Gonnelli *et al.*, cond-mat/007033.
[8] M. Nohara *et al.*, J. Phys. Soc. Jpn. **68**, 1078 (1999); M. Nohara *et al.*, Physica (Amsterdam) **341C–348C**, 2177 (2000).
[9] K. Izawa *et al.*, Phys. Rev. Lett. **86**, 1327 (2001).
[10] E. Boaknin *et al.*, Phys. Rev. Lett. **87**, 237001 (2001).
[11] In-Sang Yang *et al.*, Phys. Rev. B 62, 1291 (2000).
[12] T. Yokoya *et al.*, Phys. Rev. Lett. **85**, 4952 (2000).
[13] F. Yu *et al.*, Phys. Rev. Lett. **74**, 5136 (1995).
[14] H. Aubin *et al.*, Phys. Rev. Lett. **78**, 2624 (1997).
[15] K. Izawa *et al.*, Phys. Rev. Lett. **87**, 057002 (2001).
[16] K. Izawa *et al.*, Phys. Rev. Lett. **88**, 027002 (2001).
[17] I. Vekhter *et al.*, Phys. Rev. B **59**, R9023 (1999).
[18] K. Maki *et al.*, Physica (Amsterdam) **341C–348C**, 1647 (2000); H. Won and K. Maki, cond-mat/0004105.
[19] L. Tewordt and D. Fay, Phys. Rev. B **64**, 024528 (2001).
[20] K. Maki, P. Thalmeier, and H. Won, Phys. Rev. B **65**, 140502 (2002).
[21] P. Thalmeier and K. Maki, Acta Phys. Pol. B (to be published).
[22] V. G. Kogan *et al.*, Phys. Rev. B **60**, R12 577 (1999); S. B. Dugdale *et al.*, Phys. Rev. Lett. **83**, 4824 (1999); L. Civale *et al.*, *ibid.* **83**, 3920 (1999).
[23] C. Kübert and P. J. Hirschfeld, Phys. Rev. Lett. **80**, 4963 (1998); M. Franz, *ibid.* **82**, 1760 (1999); I. Vekhter and A. Houghton, *ibid.* **83**, 4626 (1999).
[24] G. E. Volovik, JETP Lett. **58**, 469 (1993).
[25] V. Metlushko *et al.*, Phys. Rev. Lett. **79**, 1738 (1997).
[26] We caution readers that the gap functions are rotated by 45° from those of Refs. [20,21].
[27] L. S. Borokowski and P. J. Hirschfeld, Phys. Rev. B **49**, 15 404 (1994).
[28] M. Eskildsen *et al.*, Phys. Rev. Lett. **86**, 5148 (2001).